The hydrothermal reaction of sodium molybdate, molybdenum metal, phosphoric acid, and water in a mole ratio of 6:1.2:6:57 for 90 h at 200 °C gives a 75% yield of dark crystals (pink-brown when crushed) of $Na_3Mo_2P_2O_{11}(OH)\cdot 2H_2O$.[10] The pH of the reaction mixture shortly after mixing, but before heating, is approximately 5. Simulation of the powder X-ray diffraction pattern using the coordinates from the single-crystal X-ray data solution (vide infra) shows that the product is single phase under these conditions.

The structure of **1** was determined from single-crystal X-ray data[11] and represents a new layered structure type. Views of the structure both parallel and perpendicular to the layer are shown in Figure 1. The layers, which run along (101), are composed of edge-sharing MoO_6 octahedra and corner- and edge-sharing phosphate groups. There are half as many MoO_6 dimers as phosphate tetrahedra, which gives a Mo:P ratio of 1, with two crystallographically distinct phosphate groups but only one unique MoO_6 dimer. Each MoO_6 octahedron shares three of its six corners with phosphate groups and two corners with the neighboring edge-sharing octahedron, the sixth corner being a terminal molybdenyl (Mo=O) group. The Mo–Mo distance is 2.575 (2) Å, which corresponds to a metal–metal single bond for Mo, the formulation of which is also supported by the observed diamagnetism of **1**. Each pair of MoO_6 octahedra contacts five different phosphate tetrahedra. Four of these tetrahedra each share a corner with three different dimeric MoO_6 octahedra, while the remaining phosphate group spans, via one of its edges, both oxygen atoms that are trans to the molybdenyl groups of the edge-sharing octahedra and also shares a corner with a different dimer. Both types of phosphate group have a terminal oxygen that protrudes into the interlamellar space. If an oxidation state of 5+ is assigned to the Mo, which is reasonable on the basis of the observed characteristic geometry, the calculated oxidation state from bond strength–bond length equations[12] (which gives 5 ± 0.1), and the observed diamagnetism, then there is only one H^+ per formula unit to be shared between the two terminal phosphate oxygens.[13] Inspection of the P–O bond lengths shows that there is no pronounced lengthening of the terminal P–O bond relative to the bridging oxygens but in phosphoric acid itself the terminal P–O distance is only slightly longer than that of the protonated P–O bonds (0.04–0.06 Å).

In addition to the anionic molybdenum phosphate layer framework, there are three sodium cations and two water molecules per formula unit. There are three crystallographically independent sodium cations, all of which display distorted octahedral coordination, except for Na(2), which has a seventh long Na–O bond at 2.84 Å, by oxygens with Na–O distances ranging from 2.29 to 2.79 Å. Most of these contacts are 2.3–2.5 Å and involve bonds to the phosphate oxygens and the waters of hydration. These water molecules are also involved in an extensive and complicated hydrogen-bonded network to each other and some of the layer oxygen atoms.

While the mechanisms of compound formation in the hydrothermal preparation of this and other of our reduced molybdenum phosphates[5-7] remains obscure, both pH and templating cations have large effects. Compound **1** is the only compound that we have isolated that contains a terminal but unprotonated oxygen atom, which could be due to the higher pH during this reaction. Compound **1** does not form at low pH in the presence of excess phosphoric acid.

The proton and sodium ion mobilities have been studied.[14]

Acknowledgment. We thank D. P. Goshorn for the magnetic susceptibility measurements.

Supplementary Material Available: Tables of experimental crystallographic details, derived coordinates for the atoms, anisotropic thermal parameters for the Mo, P, and Na atoms, intermolecular distances and angles, selected nonbonded contacts, and derived least-squares planes (12 pages); a listing of observed and calculated structure factors (13 pages). Ordering information is given on any current masthead page.

(10) The molybdenum powder should be <2 μm to achieve appreciable reaction rates.

(11) X-ray data for **1** (fw 551.83): monoclinic, space group $P2_1/n$ (No. 14), a = 8.128 (3) Å, b = 13.230 (4) Å, c = 11.441 (2) Å, β = 108.84°, V = 1164.4 (5) Å^3 at 23 °C, Z = 4. The calculated density is 3.15 g·cm^{-3}, λ = 0.710 69 Å, μ = 25.69 cm^{-1}, and transmission coefficients range from 0.84 to 1.00. For 121 variables and 1186 data, R (R_w) = 0.046 (0.051).

(12) Brown, I. D., Wu, K. K. *Acta Crystallogr.* **1976**, *B32*, 1957.

(13) Since the oxidation state of the Mo atoms is 5+ (see text), the extra positive charge must be present as a proton. Since the terminal phosphate oxygen is the most basic site available, it is the most likely site for the protonation. Critical inspection of the bond distances and angles around the phosphate groups and the coordinated Na^+ in question suggests a slight preference for protonation at the O(7) site. We thank a reviewer for pointing this out.

(14) Tsai, M.; Feng, S.; Greenblatt, M.; Haushalter, R. Submitted for publication.

(15) CHEM-X, designed and distributed by Chemical Design Ltd., Mahwah, NJ.

(16) Fischer, R. X. *J. Appl. Crystallogr.* **1985**, *18*, 258.

Exxon Research and Engineering Company
Annandale, New Jersey 08801

Linda A. Mundi
Robert C. Haushalter*

Received February 27, 1990

Iron–Hydroxide Stretching Resonance Raman Bands of a Water-Soluble Sterically Hindered Porphyrin

Resonance Raman (RR) spectroscopy is capable of providing important information about the strength of Fe–ligand bonds in heme proteins via the frequencies of the Fe–ligand stretching vibrational modes.[1] In particular, Fe^{III}–OH stretching RR bands have been reported at 500 cm^{-1} for alkaline horseradish peroxidase[2] and at 495 and 490 cm^{-1} for hydroxo-met hemoglobin[3] and myoglobin.[4] However, to our knowledge, no Fe–OH stretching frequency has been reported for a protein-free hydroxo-heme model complex. A principal reason is that hydroxo–Fe^{III} porphyrins have a strong propensity to condense to μ-oxo dimers in alkaline solution. Steric hindrance can inhibit dimer formation, however, and the mono(hydroxo) adduct of Fe^{III}TMP (TMP = dianion of tetramesitylporphyrin) has been reported.[5] Dimerization is also inhibited for [tetrakis(2-*N*-methylpyridiniumyl)-porphinato]iron(III)[6,7] ($Fe(T(2\text{-}N\text{-}Me)PyP)^{5+}(aq)$) complexes and is likely due to the unfavorable charge interaction as well as steric hindrance. Herein, we report the first observation and assignment of ν(Fe–OH) and ν_{sym}(Fe–$(OH)_2$) stretching bands. We have also demonstrated that the bis(hydroxo) complex constitutes an $S = {}^5/_2$, $S = {}^1/_2$ spin equilibrium that is reminiscent of alkaline met myoglobin. Hence, this water-soluble (porphinato)iron(III) complex is an interesting and pertinent model of the ligand field and Coulombic forces that govern the interplay between structure and reactivity at the prosthetic sites of heme proteins.

In Figure 1 we present isotopic evidence for the presence of two Fe–OH stretching bands in the RR spectrum of the $Fe(T(2\text{-}N\text{-}Me)PyP)^{5+}(aq)$ complex in aqueous carbonate buffer at pH 10.[8] The broad band at 541 cm^{-1} shifts to 514 cm^{-1} in $H_2{}^{18}O$, but *up* to 554 cm^{-1} in ^2H_2O. It is also apparent that the 443-cm^{-1} band is sensitive to both ^2H_2O and $H_2{}^{18}O$, although it is difficult to quantitatively evaluate the actual isotope shift because of spectral complexity. The double band may be due to a Fermi

(1) Spiro, T. G. In *Iron Porphyrins, Part Two*; Lever, A. P. B., Gray, H. B., Eds.; Addison-Wesley: Reading, MA, 1983; Chapter 3.

(2) Sitter, A. J.; Shifflet, J. R.; Terner, J. *J. Biol. Chem.* **1988**, *263*, 13032.

(3) Asher, S. A.; Vickery, L. E.; Schuster, T. M.; Sauer, K. *Biochemistry* **1977**, *16*, 5849.

(4) Debois, A.; Lutz, M.; Banerjee, R. *Biochemistry* **1979**, *18*, 1510.

(5) Cheng, R.-J.; Latos-Grazynski, L.; Balch, A. L. *Inorg. Chem.* **1982**, *21*, 2412.

(6) Kobayashi, N. *Inorg. Chem.* **1985**, *24*, 3324.

(7) Chen, S.-M.; Sun, P.-J.; Su, Y. O. Submitted for publication.

(8) Although the pH transitions are sensitive to the presence of coordinating anions other than hydroxide, the ν(Fe–OH) and ν_{sym}(Fe–$(OH)_2$) stretches are not.

0020-1669/90/1329-2881$02.50/0

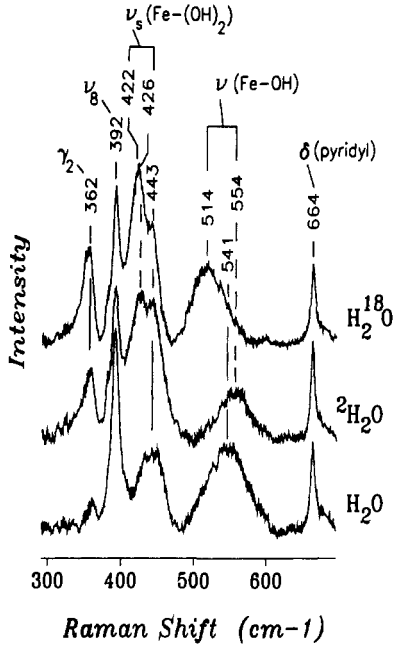

Figure 1. Resonance Raman spectra of the low-frequency region (465.8-nm Ar^+ laser excitation) of 1 mM Fe^{III}(T(2-*N*-Me)PyP)$^{5+}$(aq) solutions[23] (carbonate buffer) at pH 9.9. Solution pH was adjusted by dissolving carbonate buffer solid in the appropriate water isotope. A standard spinning NMR tube (5 mm) 135° backscattering geometry was used. The scattered light was dispersed with a Spex Triplemate monochromator (2400 groove/mm grating) and collected with a Princeton Instruments optical multichannel analyzer. Typical laser powers were 25 mW.

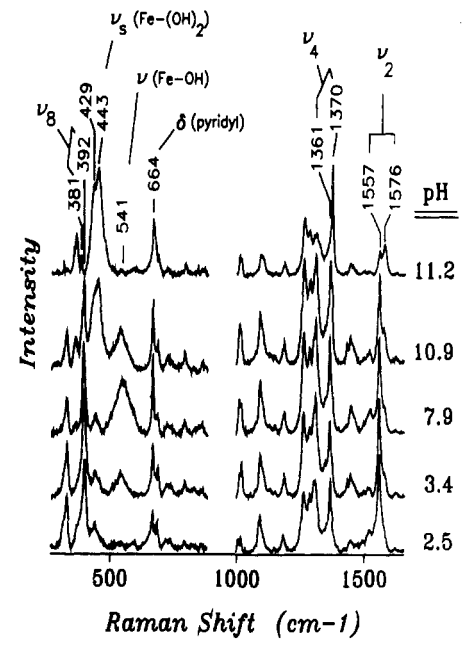

Figure 2. Resonance Raman spectra of low-frequency (465.8-nm Ar^+ laser excitation) and high-frequency (441.6-nm HeCd laser excitation) regions of 1 mM Fe^{III}(T(2-N-Me)PyP)$^{5+}$(aq) solutions (in 0.2 M $NaClO_4$) at pH 2.5, 3.4, 7.9, 10.9, and 11.2. Solution pH was adjusted by adding either NaOH or $HClO_4$ to exclude the presence of other coordinating anions. A standard spinning NMR tube (5 mm) 135° backscattering geometry was used. The scattered light was dispersed with a Spex Triplemate monochromator (2400 groove/mm grating) and collected with a Princeton Instruments optical multichannel analyzer. Typical laser powers were 25 mW.

resonance with an interacting porphyrin mode or to heterogeneity introduced by the presence of several rotational isomers of the 2-*N*-methylpyridiniumyl rings.[9] The remaining bands of the spectrum are pyridyl or porphyrin modes,[10,11] including the 361-cm^{-1} band, which shows a 4-cm^{-1} downshift in $H_2{}^{18}O$. The intensity change of this band tracks that of the 443-cm^{-1} band in the pH titration (Figure 2), and it is tentatively assigned to an out-of-plane mode that is coupled to the Fe–OH stretch. The pyrrole swiveling mode γ_2, which has been assigned at 330 cm^{-1} in NiTPP,[18] is a likely candidate. (This band is *not* the Fe–O–Fe mode of the residual μ-oxo dimer, which is expected at about the same frequency[13] but is not ^{18}O sensitive, and has negligible intensity in these solutions.)

Spectroscopic pH titrations permit us to identify the 541-cm^{-1} band with a 5-coordinate high-spin Fe^{III} adduct and the 443-cm^{-1} band with a low-spin 6-coordinate bis(hydroxide). Figure 2 shows the 541-cm^{-1} band growing in as the pH is raised from 2.5 to neutrality. This band diminishes at higher pH and disappears above pH 11. In contrast, the 443-cm^{-1} band only appears through the high-pH transition. The latter transition also produces changes

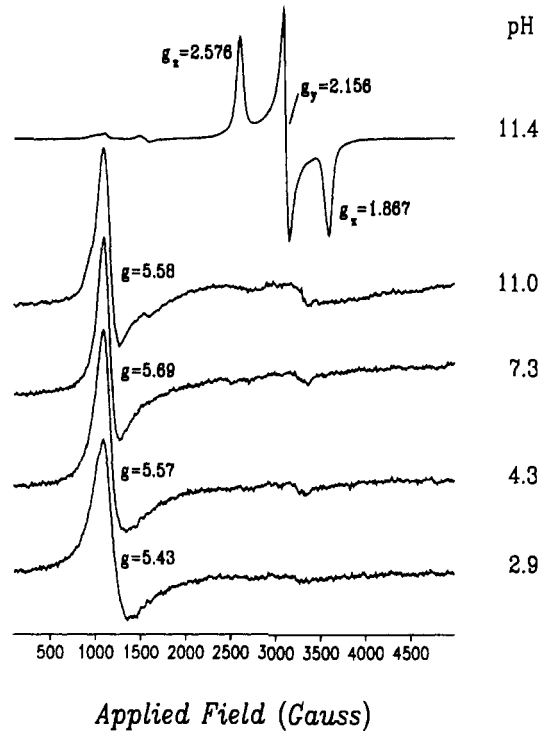

Figure 3. X-Band ESR spectra of Fe^{III}(T(2-*N*-Me)PyP)$^{5+}$(aq) solutions (in 0.2 M $NaClO_4$) at pH 2.9, 4.3, 7.3, 11.0, and 11.4, acquired at 9.35 GHz. Acquisition parameters were as follows: T = 120 K, 1024 points, 100-kHz modulation frequency, 10-G modulation amplitude, 6000-G sweep width (only 100–5000 G shown). Solution pH was adjusted by adding either NaOH or $HClO_4$.

in the high-frequency region of the spectrum, where bands sensitive to the spin state are found.[10] In particular, the strong bands at 1361 and 1557 cm^{-1} diminish through the pH 11 transition and are replaced by bands at 1370 and 1576 cm^{-1}. These pairs of

(9) Collman, J. P.; Gagne, R. R.; Reed, C. A.; Halbert, T. R.; Land, G.; Robinson, W. T. *J. Am. Chem. Soc.* **1975**, *97*, 1427.
(10) Spiro, T. G.; Li, X.-Y. In *Biological Applications of Raman Spectroscopy*; Spiro, T. G., Ed.; John Wiley & Sons: New York, 1988; Vol. III, Chapter 1.
(11) Blom, N.; Odo, J.; Nakamoto, K.; Strommen, D. P. *J. Phys. Chem.* **1986**, *90*, 6083.
(12) Li, X.-Y.; Czernuszewicz, R. S.; Kincaid, J. R.; Su, Y. O.; Spiro, T. G. *J. Phys. Chem.* **1990**, *94*, 31.
(13) Burke, J. M.; Kincaid, J. R.; Spiro, T. G. *J. Am. Chem. Soc.* **1978**, *100*, 6077.
(14) Burke, J. M.; Kincaid, J. R.; Peters, S.; Gagne, R. R.; Collman, J. P.; Spiro, T. G. *J. Am. Chem. Soc.* **1978**, *100*, 6083.
(15) Palmer, G. In *Iron Porphyrins, Part Two*; Lever, A. P. B., Gray, H. B., Eds.; Addison-Wesley: Reading, MA, 1983; Chapter 2.
(16) La Mar, G. N.; Walker, F. A. In *The Porphyrins*; Dolphin, D., Ed.; Academic Press: New York, 1979; Vol. IV, Chapter 2.
(17) Shiemke, A. K.; Loehr, T. M.; Sanders-Loehr, J. *J. Am. Chem. Soc.* **1986**, *108*, 2437.
(18) Calculations were done on a VAX 11-780 computer, using GMAT and FPERT from National Research Council of Canada Bulletin No. 15, 1975, by K. G. Kidd et al.

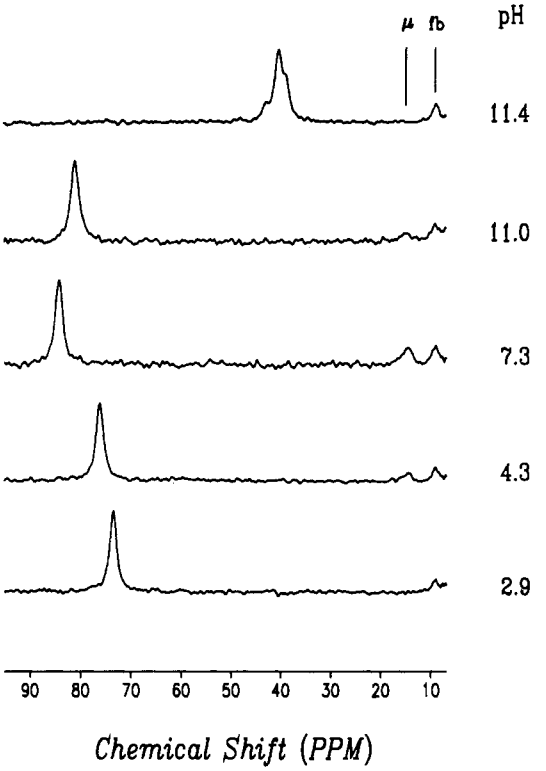

Figure 4. ^{2}H NMR spectra of 1 mM $Fe^{III}(T(2\text{-}N\text{-}Me)PyP)^{5+}$(aq) solutions (in 0.2 M $NaClO_4$) at pH 2.9, 4.3, 7.3, 11.0, and 11.4, acquired at 38 MHz in a 10-mm tube at ambient temperatures. The spectra contained 8K data points over a spectral window of 10 kHz. Solution pH was adjusted by adding either NaOH or $HClO_4$. Minor contributions from free base (fb) and iron μ-oxo dimer (μ) are indicated.

frequencies are characteristic of high- and low-spin Fe^{III} species,[12] respectively. The ESR spectrum (Figure 3) is characteristic of a high-spin Fe^{III} ($g = 6$ and 2) species until the titration approaches the second equivalence point. Low-spin features then appear in the spectrum and beyond pH 11. The spectrum indicates nearly all low-spin Fe^{III} ($g_z = 2.54$, $g_y = 2.15$, $g_x = 1.90$) at 120 K.[15] ^{2}H NMR spectra of the β-deuterated pyrrole complex (Figure 4) show a resonance shifting from 73.5 ppm at pH 2.9 to 84 ppm at pH 7.3, indicating conversion from one high-spin Fe^{III} species to another,[16] while at pH 11.4 the resonance is a multiplet between the high-spin values and a typical low-spin value (−20 to −30 ppm).[16] Curie plots for these signals exhibit a negative slope and are consistent with a spin equilibrium at pH 11.4. Likewise, the RR spectrum at this pH shows both low- and high-spin porphyrin marker bands. The low-spin ESR spectrum (Figure 3), taken at 120 K, reflects the low-spin character of the ground state at this temperature.

These data are consistent with previous spectrophotometric titrations of this complex,[6,7] which indicate pK_a values of ~5 and ~11. Kobayashi[6] had similarly inferred high-spin character for the acid and neutral species, assigned to the aquo- and mono(hydroxo) complexes, respectively, and low-spin character for the high-pH complex, assigned to the bis(hydroxide). Our data indicate that the latter species constitutes a spin-state equilibrium at room temperature. The assignment of the 443-cm^{-1} Fe-OH stretch to the low-spin component of this mixture is based on the observation that this band persists at low temperature (data not shown).

The 27-cm^{-1} ^{18}O downshift of the 541-cm^{-1} mono(hydroxo) band (Figure 1) is as expected for an Fe–OH oscillator, but the 13-cm^{-1} upshift in D_2O is surprising; an 11-cm^{-1} downshift would be expected on the basis of a diatom calculation with point mass 17 (OH) and 18 (OD) oscillators. A similar upshift has been noted in hemerythrin,[17] however, and was attributed to coupling with the Fe–O–H bending mode. We have been able to model the upshift with a bent (110°) Fe–O–H oscillator having Fe–O and O–H stretching force constants of 2.3 and 5.13 mdyn/Å, a bending force constant of 0.2 mdyn Å/rad^2 and a stretch–bend interaction constant of 0.07 mdyn/Å.[18] The bending mode is calculated to be 614 cm^{-1} for Fe–OH and 437 cm^{-1} for Fe–OD, thus crossing over the Fe–OH stretch and producing the upshift via kinematic coupling.

The stretching frequency is higher for the high-spin mono(hydroxo) than the low-spin bis(hydroxide) complex. Part of this effect arises from altered kinematics, as the bis(hydroxide) stretching mode is the symmetric stretch in which the central Fe atom does not move, but part of it stems from a higher force constant for the mono(hydroxo) complex. A linear triatom calculation with point mass OH ligands gives a stretching force constant of 2.0 mdyn/Å for the bis(hydroxide) complex. This value is quite reasonable for low-spin Fe^{III}. For comparison, the force constant is 1.6 mdyn/Å for the bis(imidazole) adducts of both Fe^{III} and Fe^{II} porphyrins.[19] Why then is the mono(hydroxo) force constant even larger, 2.3 mdyn/Å, despite the Fe^{III} being high-spin? The answer may lie in the ability of the single hydroxide ligand to polarize the iron orbitals. High-spin Fe^{III} has a half-occupied d_{z^2} orbital, which is formally antibonding with respect to the axial ligand. The d_{z^2} electron can, however, be concentrated on the back side of the 5-coordinate complex, via $3d_{z^2}$–$4p_z$ hybridization. This permits the hydroxide σ electrons unimpeded access to the Fe^{III} ion, and in addition, the hydroxide π electrons can engage in donor interactions with the filled Fe^{III} d_π orbitals. Strong bonding in high-spin 5-coordinate Fe^{III} adducts finds precedence in the case of the fluoride[3,20] and methoxide[21] complexes.[22] These arguments imply that the aqueous mono(hydroxo) complex is predominantly five-coordinate and that a water molecule is at most loosely bound as a sixth ligand.

The RR, NMR, and ESR data provide consistent and compelling evidence for the existence of primarily three coordination states of the $Fe(T(2\text{-}N\text{-}Me)PyP)^{5+}$(aq) ion in solutions of varying pH: a high-spin aquo complex at low pH, a high-spin 5-coordinate mono(hydroxo) complex at intermediate pH, and a high-spin/low-spin equilibrium of bis(hydroxide) species at high pH.

Acknowledgment. This work was supported by U.S. Department of Energy Grant DE-ACO-81ER10861 (T.G.S.) and the National Science Council of the Republic of China (Y.O.S.). R.A.R. (GM12197-02) and K.R.R. (1 F32 HL08116-01) are recipients of NIH National Research Service Awards.

(19) Mitchell, M. L.; Li, X.-Y.; Kincaid, J. R.; Spiro, T. G. *J. Phys. Chem.* **1987**, *91*, 4690.
(20) Kincaid, J.; Nakamoto, K. *Spectrosc. Lett.* **1976**, *9*, 19.
(21) Lecomte, C.; Chadwick, D. L.; Coppens, P.; Stevens, E. D. *Inorg. Chem.* **1983**, *22*, 2982.
(22) The axial ligand stretching frequency[20] (600 cm^{-1}) and force constant[3] (2.9 mdyn/Å) of the fluoride adduct are high and the Fe^{III}–O bond is short, 1.816 Å, in the methoxide adduct.[21]
(23) Prepared by the method of: Davila, J.; Harriman, A.; Richoux, M.-C.; Milgrom, L. R. *J. Chem. Soc., Chem. Commun.* **1987**, 525.

Department of Chemistry
Princeton University
Princeton, New Jersey 08544

Robert A. Reed
Kenton R. Rodgers
Kristine Kushmeider
Thomas G. Spiro*

Department of Chemistry
National Taiwan University
Taipei, Taiwan 10764

Y. Oliver Su*

Received December 27, 1989

Soluble and Volatile Yttrium and Copper Alkoxo–Acetylacetonato Derivatives. Synthesis and Crystal Structure of $Y_3(\mu_3,\eta^2\text{-}OC_2H_4OMe)_2(\mu_2,\eta^2\text{-}OC_2H_4OMe)_2(\mu_2,\eta^1\text{-}OC_2H_4OMe)(acac)_4$

The synthesis of high-tech materials by chemical routes such as sol–gel technology[1] or chemical vapor-phase decomposition[2]

